MiHATP:A Multi-Hybrid Attention Super-Resolution Network for Pathological Image Based on Transformation Pool Contrastive Learning –Supplementary Material-

1 Method Appendix

Algorithm 1 algorithm of MiHATP

Input: $\{I^{LR}\}$.
Input: $\theta = \{\theta_{base}, \theta_{con}, \theta_{extract}\}$, initial parameters.
Output: $\{I^{SR}, r_i^l\}_{i=1}^N\}$, high-resolution image and high-resolution representation

for $t \in 1, 2, ..., epochs$ **do**
  for $i \in 1, 2, ..., N$ **do**
    $I_i^{SR} \leftarrow F_{base}\ (I_i^{LR}; \theta_{base}\ )$
    $X_i^P \leftarrow \{P_j | P_j \leftarrow T_{inv}(F_{con}(T_{for}(I_i^{LR}); \theta_{con}))\}_{j=1}^{K_p}$
    $X_i^N \leftarrow \{N_j | N_j \leftarrow T_{irr}(I_i^{HR})\}_{j=1}^{K_n}$
    $\{r_i^l\}_{i=1}^N \leftarrow Resnet(I_i^{SR}; \theta_{extract})$
    $\{p_i^{l,k}\}_{k=1}^{K_p} \leftarrow Resnet(X_i^P; \theta_{extract})$
    $\{n_i^{l,j}\}_{l=1}^{K_n} \leftarrow Resnet(X_i^N; \theta_{extract})$
    calculate $Loss_{total}$
    $\theta \leftarrow \theta - \eta \cdot \nabla Loss_{total}$
  end for
end for
return $\{I^{SR}, r_i^l\}_{i=1}^N\}$

2 Experiment Appendix

Implementation Settings					
Device	MiHATP			Feature Extraction Network	
	M-RHAG	M-HAB	Window size	Type	Depth
Nvidia A100 GPU	6	6	8	Resnet50	4

In our experiment, we configure six M-RHAG modules in MiHATP, with each M-RHAG containing six M-HAT modules.Following the output of the super-resolution network for super-resolution image, we append a pre-activated ResNet50 to construct a downstream task-friendly feature extraction network. However, we omit the first pooling layer of ResNet to prevent premature loss

of important information in the sampled super-resolution images. The number of layers L in the feature representation network is set to 4. All methods are implemented in Python using PyTorch and trained on an Nvidia A100 GPU with 80GB memory. Here we present additional super-resolution results at an

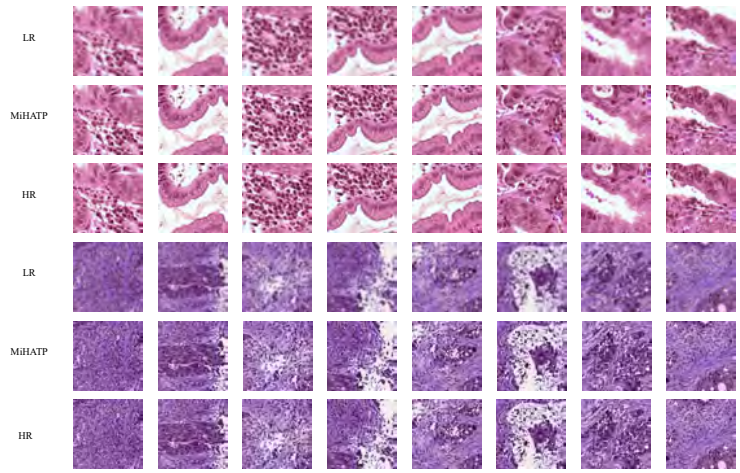

Fig. 1. More super-resolution images generated by MiHATP.

x4 scale, showcasing various tissue regions. This figure clearly demonstrates the excellent representational capability of MiHATP across different regions.

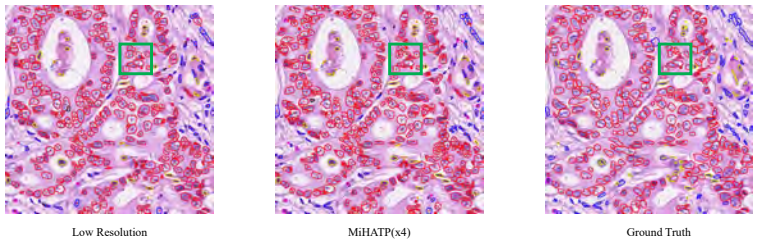

Fig. 2. The output of Hover-Net.

Here, we present a comparison between the super-resolution images generated by MiHATP, high-resolution images, and low-resolution images processed using Bicubic interpolation under Hover-Net. The green boxes highlight noticeable improvements. In densely overlapping cellular regions, MiHATP demonstrates better characterization of local cell edges and boundaries between different cells.